Direct Determination of Primary Cosmic-Ray Alpha-Particle Energy Spectrum by New Method*

FRANK B. McDONALD
Department of Physics, State University of Iowa, Iowa City, Iowa
(Received March 30, 1956; revised manuscript received June 13, 1956)

The flux of cosmic-ray alpha particles has been measured at $\lambda=41°$N and 55°N and the energy spectrum in the region 883–285 Mev/nucleon has been determined by the use of a combination of a scintillation and Čerenkov counter. This spectrum is not dependent on geomagnetic theory. It has been found that the integral alpha spectrum can be fitted with the function

$$J_{0\alpha}(E)=\frac{431}{(1+E)^{1.4\pm0.2}}\ \text{particles/m}^2\text{-sec-sterad},$$

and

$$J_{0\alpha}(E_1)=87\pm9\ \text{particles/m}^2\text{-sec-sterad},\quad \lambda=41°\text{N},$$
$$J_{0\alpha}(0.285\ \text{Bev})=292\pm25\ \text{particles/m}^2\text{-sec-sterad},\quad \lambda=55°\text{N}.$$

$J_{0\alpha}(E)$ is the flux of α particles at the top of the atmosphere with kinetic energy $\geqq E$ (in Bev/nucleon). E_1 is the cutoff energy/nucleon for α particles at 41°N. An absorption mean free path $\lambda_\alpha=45\pm7$ g/cm² has been measured for alpha particles. The properties of this new detector are discussed and a study is made of the energy response of the Čerenkov counter to fast multiply-charged particles.

I. INTRODUCTION

RECENTLY it has been demonstrated[1–3] that it is possible to obtain consistent and accurate flux values of the low-Z components of the primary cosmic radiation by using Čerenkov counters at low latitudes. However, it appears impossible to extend these measurements to higher latitudes since, with the Čerenkov counter, slow particles of high Z give pulses equivalent to those of fast particles of lower charge. If such an extension were possible, it would be of great interest since the region from 41° to 55° geomagnetic latitude covers the velocity-sensitive region of the average Čerenkov counter, and it should make possible the direct determination of the energy spectrum of various components without having the uncertainties introduced by combining the geomagnetic theory with a latitude survey. In addition, an electronic detector has great advantages in the study of time variations at high latitudes. Many investigators have proposed that the combination of a Čerenkov counter and an ionization device would provide a means of extending the range of the Čerenkov counter, and indeed, might be an instrument with greatly improved charge and velocity resolution. Calculations to this effect were first carried out by Linsley.[1] The ionization device has for the most probable energy loss a response of the form[4]:

$$\epsilon_p=\frac{2Z^2m_ec^2Cx}{\beta^2}\left[\ln\left(\frac{4Cm_e^2c^4xZ^2}{(1-\beta^2)I^2(Z_1)}\right)-\beta^2+J\right], \quad (1)$$

$$C=0.150Z_1/A_1.$$

In this formula, Z and β are the charge and velocity of the incident particle, Z_1 and A_1 are the charge and mass number of the stopping material, x is the thickness of the crystal in g/cm², and J is a small correction factor which is a function of β, Z, and x. $I(Z_1)$ is the average ionization potential of the medium, and the other symbols are standard. For the Čerenkov counter[5] the number of photons per cm, dN, emitted between wavelengths λ and $\lambda+d\lambda$ in a medium with an index of refraction n by a particle of velocity β and charge Z, is

$$dN=\frac{2\pi Z^2d\lambda}{137\lambda^2}\left(1-\frac{1}{\beta^2n^2}\right). \quad (2)$$

It will be noted that for the Čerenkov detector the output signal, N_c, is decreased as the velocity is decreased, while for the ionization detector the output

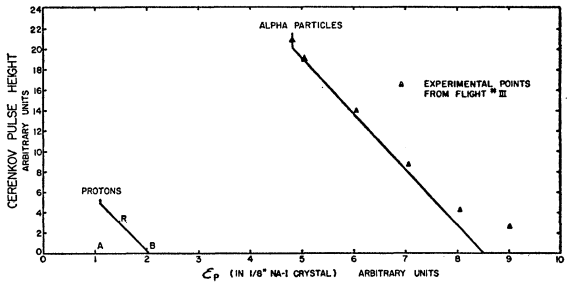

FIG. 1. Plot of Čerenkov pulse height in 1-in. Lucite radiator *vs* the most probable energy loss for protons and alphas in a ⅛-in. NaI crystal. Fast albedo particles will be along *A–B*. *R–B* represents particles below geomagnetic cutoff. Triangles represent observed response of Čerenkov detector to fast multiply-charged particles in Flight III.

* Assisted by the joint program of Office of Naval Research and the U. S. Atomic Energy Commission.

[1] J. Linsley, Phys. Rev. **97**, 1292 (1955).
[2] N. Horowitz, Phys. Rev. **98**, 165 (1955).
[3] W. R. Webber and F. B. McDonald, Phys. Rev. **100**, 1460 (1955).
[4] K. R. Symon, thesis, Harvard University, 1948 (unpublished); see also B. Rossi, *High-Energy Particles* (Prentice-Hall, Inc., New York, 1952), Sec. 2.7.
[5] L. I. Schiff, *Quantum Mechanics* (McGraw-Hill Book Company, Inc., New York, 1949), p. 265.

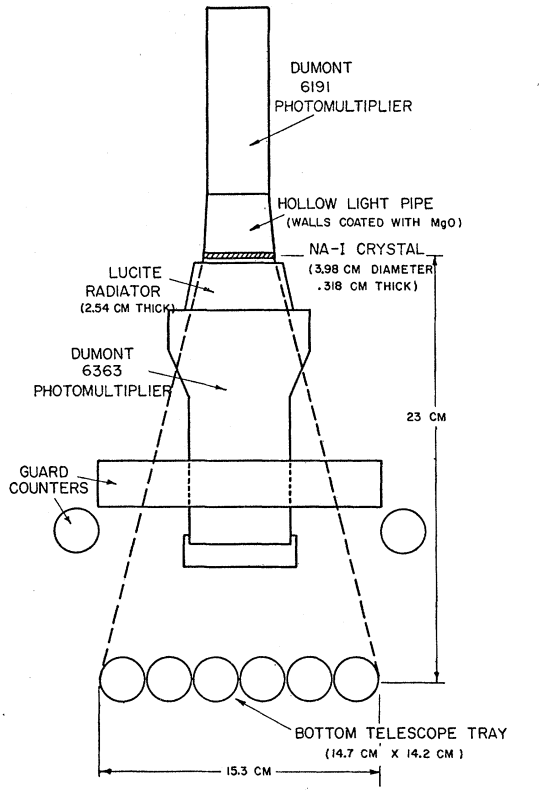

FIG. 2. Schematic drawing of telescope.

signal is increased as the velocity is decreased. In Fig. 1, a plot is given of the response of such a combination of these two types of detectors to protons and alpha particles in the energy range above 320 Mev/nucleon. For energies less than 1 Bev/nucleon, the curve of ϵ_p *vs* N_c can be represented by

$$N_c = Z^2 K_1 - K_2 \epsilon_p, \tag{3}$$

where K_1 and K_2 are constants. With the individual detectors, resolution of the cosmic-ray charge spectrum is possible only for relativistic particles. However,

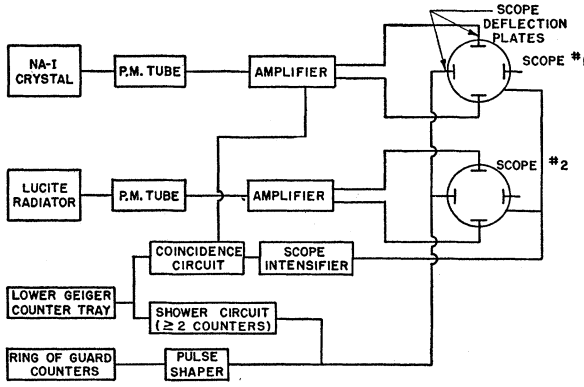

FIG. 3. Schematic diagram of electronic circuits.

Fig. 1 demonstrates that the combination of these two types of detectors gives charge resolution which is independent of velocity. This resolution will be extended below the Čerenkov threshold because of material in the telescope beneath the ionization detector. In the present experiment incident particles must have an energy greater than 120 Mev/nucleon. This prevents slow protons from extending into the nonrelativistic alpha region. Since the response of both detectors is velocity-dependent, it follows that if effective charge resolution can be achieved, it will also be possible to obtain a velocity spectrum of the various Z components of the cosmic radiation in the range 1 Bev to 100 Mev. This determination of the energy spectrum would depend only on the properties of the detector and would be independent of geomagnetic theory. In addition other useful information would be obtained. Because of the directional properties of the Čerenkov counter, particles lying along the line A–B in Fig. 1 would represent the upward moving albedo of the cosmic radiation, and it would be possible to gain some idea of the energy distribution of these particles. The particles lying along R–B, where R is at the vertical geomagnetic cutoff energy, would represent most of the protons in the returning albedo and slow secondaries generated in the atmosphere.

Detectors using this principle have been developed at the State University of Iowa, and three flights using Skyhook balloons have been completed. Two flights were made at $\lambda = 41°$N (San Angelo, Texas). One flight was made at $\lambda = 55°$N (Minneapolis, Minnesota) on July 7, 1955. These initial flights were made to measure the proton and alpha-particle flux. Further flights are planned at 58°, 55°, and 52° to study $Z = 1-6$ components. The results of the flight at $\lambda = 55°$N dealing with alpha particles, in addition to related data from the $\lambda = 41°$N flights, will be discussed in this paper. The data on primary protons and cosmic-ray albedo will be discussed in a future paper.

II. APPARATUS

A schematic drawing of the telescope is given in Fig. 2. The telescope geometric factor is 4.02 ± 0.15 cm² sterad for Flight III and 7.25 ± 0.3 cm² sterad for Flight I. Figure 3 gives a schematic drawing of the electronic circuits. A coincidence is formed when there is a simultaneous pulse from the Geiger counter tray and a pulse greater than 0.5 × the most probable energy loss for a proton at minimum ionization in the crystal channel. The pulses from the lower Geiger counter tray also actuate a shower circuit so that there is an indication on the horizontal cathode ray tube plates when an event occurs and more than one counter in the lower tray is discharged. A ring of guard counters is placed above the lower tray to assist in the detection stars and side showers and to provide better definition of the telescope geometric factor.

III. DETECTOR RESOLUTION

The sea-level cosmic-ray mu mesons are convenient particles for checking the resolution of the telescope. In actual practice, particles of a given charge will not lie along one of the lines shown in Fig. 1, but will be distributed in a region about this line because of various types of fluctuations. In the scintillation counter the principal fluctuation is the Williams-Landau effect. This fluctuation arises when fast charged particles traverse a thin absorber since large energy transfers to single electrons can occasionally occur. The most probable energy loss, ϵ_p, is given by Formula (1) and there is a straggling of the individual losses around this value. The curves presented in Symon's[4] thesis are used in the calculation on fluctuations in energy loss. Figure 4 gives an observed pulse-height distribution for sea-level mu mesons and the predicted curve based on the Williams-Landau effect. It is seen that excellent agreement with the predicted curve is obtained on the high-energy side of the curve. In Fig. 5 is shown

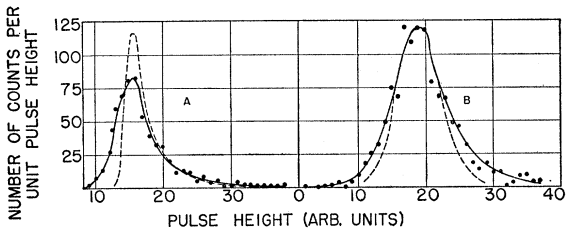

FIG. 4. (a) The solid circles and line give the experimental pulse height distribution for sea level mu mesons in a 1.16-g/cm² NaI crystal. The dashed line is the calculated curve for a Williams-Landau distribution. (b) Experimental sea-level mu meson pulse height distribution in Lucite Čerenkov detector. The dashed line represents a Poisson distribution with $\bar{n}=34$.

the calculated Williams-Landau distribution for α particles with energies of 4, 1.5, 0.8, 0.4, 0.3, and 0.2 Bev/nucleon. The distributions become more Gaussian in shape and become progressively sharper as the kinetic energy of the particles is decreased. Figure 4 also gives the experimental Čerenkov distribution for sea-level mu mesons. It is seen that the observed distribution is asymmetric. This represents an effect in the Čerenkov counter similar to the Williams-Landau effect in an ionization detector.

IV. FLIGHT DATA

The time-altitude data for Flight I at $\lambda=41°$ (San Angelo, Texas) on January 17, 1955 and Flight III at $\lambda=55°$ (Minneapolis, Minnesota) on July 7, 1955, are given in Fig. 6.

Reduction of the data was carried out by displaying the film on a Model C Recordax microfilm reader and, for each event, measuring the pulse height in the Čerenkov channel and in the ionization channel. The data were tabulated on a 40×40 rectangular array.

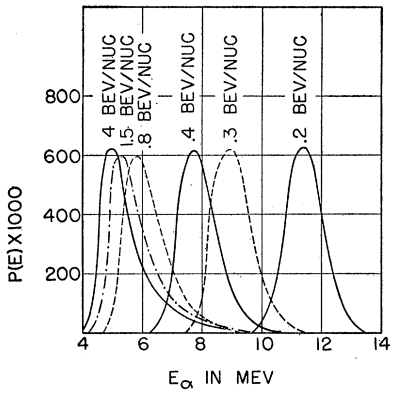

FIG. 5. Calculated Williams-Landau distribution for alpha particles of 1.5, 0.8, 0.4, 0.3, and 0.2 Bev/nucleons. $P(E)$ represents the probability of energy loss E in the crystal by a particle of given energy.

After the film data had been transferred to the 40×40 array, it was divided into various ionization intervals and the Čerenkov distributions in these intervals were studied. This is illustrated in the uncorrected data of the α-particle region given in Fig. 7. These give the the distribution of the regular Čerenkov counts in the selected ionization intervals and the distribution of the multiple particle counts. No corrections have been applied. It is felt that the good peak-to-valley ratio, the sharp falloff on the higher side of the distribution, and the multiple-particle pulse distribution indicate a minimum of background in the alpha region. This is further strengthened by the observed altitude dependence given in Fig. 8 which will be discussed later.

V. CORRECTIONS IN ALPHA REGION

There are four corrections to be applied to the observed alpha data in order to deduce an absolute flux at the top of the atmosphere. There are: a general background correction, a correction for the absorption of alpha particles in the telescope and in the atmosphere above the telescope due to nuclear interactions, a δ-ray correction, and a correction for the production of alphas in the atmosphere by the fragmentation of primary heavy nuclei.

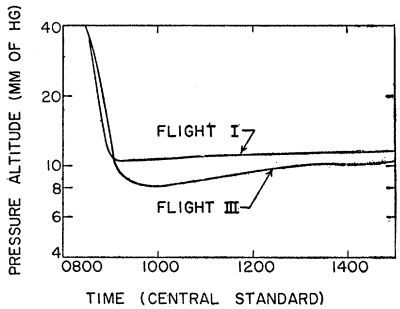

FIG. 6. Time altitude curve for Flight I (San Angelo, Texas, January 17, 1955) and Flight III (Minneapolis, Minnesota, July 7, 1955).

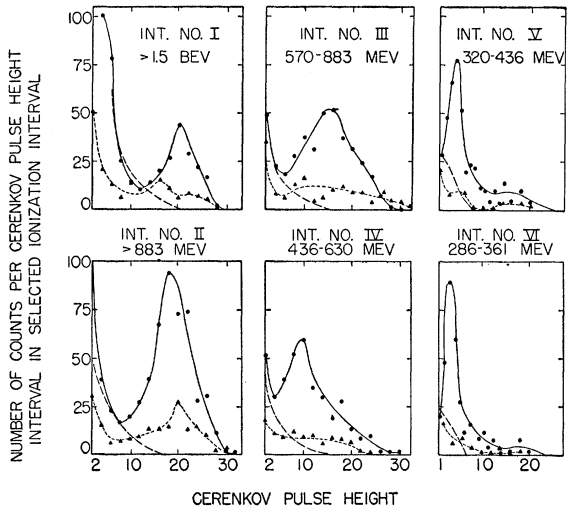

FIG. 7. The solid circles and lines give raw differential pulse height data, in selected ionization intervals. The heavy dashed line represents background counts in the interval. The triangles and dashed line gives the distribution of J counts in the interval. The ordinate scale represents the actual number of counts at altitude.

The shape of the background correction is taken to be the interval at $3\times\epsilon_p$ for protons at minimum ionization. In Fig. 1 this corresponds to a line drawn parallel to the ordinate and intersecting the abscissa at 3.6 on the arbitrary scale. The ionization distribution rises rapidly so it is possible to select a region just behind a group of particles with the desired charge and this region will be almost completely free of particles having this charge. The flight at $\lambda=41°$N demonstrated that the shape of the background curve did not change across the complete alpha interval. The background curve obtained at $\lambda=55°$N was normalized on the low-energy side of the Čerenkov distributions. The corrections to the various intervals by this method are given in Fig. 7.

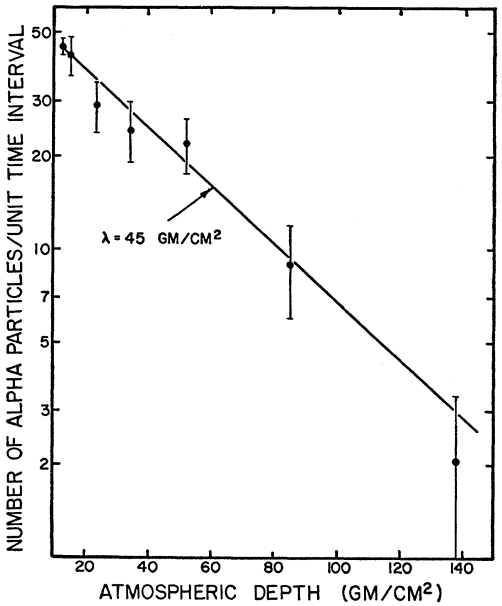

FIG. 8. Vertical intensity of alpha particles as a function of atmospheric depth. This gives an apparent mean free path of 45 ± 7 g as indicated by the solid line.

In order to correct for the attenuation of the α particles by nuclear interactions, it is necessary to know the interaction mean free path, λ_α. A value of 45 ± 7 g/cm^2 is obtained from the observed atmospheric absorption (Fig. 8) of α's in Flight III. This is in agreement with the values of λ_α obtained by Waddington,[6] Quarenti and Zorn,[7] and Webber and McDonald.[3]

The δ-ray correction is necessary, as it is possible for particles traversing the top two elements of the telescope to produce knock-on electrons which will trigger one of the Geiger counters. For particles which would normally pass through the telescope, this results in their being classified as multiple particle counts. Some particles which miss the bottom element will appear as regular counts and there will be a spurious increase of the geometric factor. Details of this calculation have been given by Webber and McDonald.[3] At energies below 800 Mev/nucleon, this correction becomes negligible.

To extrapolate the observed alpha flux to the top of the atmosphere, it is also necessary to correct for the production of energetic particles by the fragmentation of heavy nuclei above the telescope. This is similar to the correction required in the Li, Be, and B region. The fragmentation probabilities derived by Noon and Kaplon[8] have been used to obtain the number of secondary α's incident on the telescope. At $\lambda=55°$ the number of secondary alphas as 12 g/cm^2 is 11 ± 4 particles/m^2-sec-sterad. At $\lambda=41°$ the number of secondary alphas at 15 g/cm^2 is 6.5 ± 3 particles/m^2-sec-sterad. This correction has not been applied to the differential and integral spectrum in Figs. 9 and 10.[9]

VI. ENERGY CALIBRATION

The selected intervals of ionization were calibrated in terms of the most probable energy loss for α particles at minimum ionization, $(\epsilon_p)_{\alpha\,\min}$. From the data at $\lambda=41°$ it is known that some 25% of the alphas at 55° will have energies greater than 2 Bev/nucleon and will be at minimum ionization. The ionization distribution of these particles can be studied by selecting an interval along the high side of the Čerenkov distribution. In Fig. 1 this corresponds to taking an interval parallel to the ϵ_p axis and intersecting the Čerenkov axis at 21. This gives a pulse-height dis-

[6] C. J. Waddington, Phil. Mag. **45**, 1312 (1954).
[7] G. T. Quarenti and G. T. Zorn, Nuovo cimento **1**, 1282 (1955).
[8] J. H. Noon and M. F. Kaplon, Phys. Rev. **97**, 769 (1955).
[9] Complete details on all corrections can be obtained from the State University of Iowa Physics Department Report, SUI 56-4 (unpublished).

TABLE I. Summary of α-particle data for Flights I and III.

Flight III. $\lambda = 550$

Interval	dE/dX in crystal in Mev	Energy interval defined at 12 g residual atmosphere Mev/nucleon	Energy interval corrected to top, of atmosphere Mev/nucleon	N (No. of α counts in interval)	N_α with Landau-Williams correction	J_α at 12 g/cm² (particles/m²-sec-sterad per unit interval)	$J_{0\alpha}$ (particles/m²-sec-sterad per unit interval)	$dJ_{0\alpha}/dE$ (number of α's/m²-sec-sterad Mev)
I and II	<5.68	>855	>883	525	784	108	182	
III	5.68–6.70	540–855	570–883	348	190	26.0	42.5	0.136±0.02
IV	6.45–7.75	398–600	436–630	285	202	27.8	45.5	0.24 ±0.03
V	7.75–9.30	278–398	320–436	166	145	20.0	32.6	0.28 ±0.045
VI	8.52–10.06	241–328	286–360	134	118	16.3	26.7	0.36 ±0.06

Flight I. $\lambda = 41°$

N_α (No. of alpha counts)	J_α at detector (particles/m²-sec-sterad)	$J_{0\alpha}$ [particles/m²-sec-sterad at top of atmosphere (without fragmentation correction)]	$J_{0\alpha}$ [particles/m²-sec-sterad at top of atmosphere (with fragmentation correction)]
460±22	56.0	96±8	87±9

tribution similar to that shown in Fig. 4. The peak in the distribution thus obtained is $(\epsilon_p)_{\alpha\,\min}$, and the values of $(\epsilon_p)_\alpha$ of the other intervals are known in terms of $(\epsilon_p)_{\alpha\,\min}$ since the system is a linear one. The peak in the ionization distribution is quite accurately defined and the position of $(\epsilon_p)_{\alpha\,\min}$ on the 40×40 array is known to 3%. The data relevant to the energy calibration are summarized in the first four columns of Table I. Thus the energy calibration is furnished by the relativistic alphas as defined by the Čerenkov counter, and the calibration of the system is provided internally and does not depend on preflight calibration. Because of the accuracy of the determination of $(\epsilon_p)_{\alpha\,\min}$ and the linearity of the system, it is estimated that the energies defined by the intervals are known to ±5%. The extrapolation of these intervals to the top of the atmosphere was carried out by using standard range-energy relations[10] for alpha particles in air.

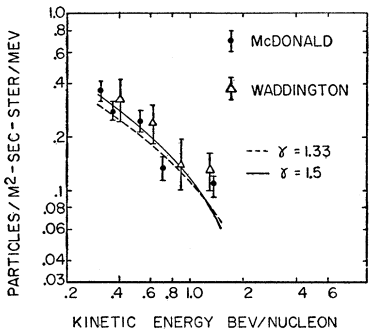

FIG. 9. Differential energy spectrum for primary alpha particles. The emulsion data obtained by Waddington[11] are shown for comparison. The data have been fitted to a curve of the form $J(\geqq E) = c/(1+E)^\gamma$. The point on the right at 1.3 Bev was obtained by using data at $\lambda = 41°$. This is the only point involving geomagnetic theory and was disregarded in fitting the data.

[10] *Range Energy Curves*, U. S. Atomic Energy Commission Report AECU-663 (unpublished).

VII. ALPHA-ENERGY SPECTRUM

To derive an energy spectrum from the distributions given in Fig. 7, it is necessary to relate the observed number of particles within an interval of energy loss to the actual number in the corresponding energy interval. The calibration of the energy intervals in terms of ionization loss was discussed in the previous section. However, due to fluctuations introduced by the detectors, the number of particles within an interval of energy loss is not necessarily the number in the related energy interval. The largest correction will be the Williams-Landau correction for high-energy alphas. It is a major correction only in the energy region $\geqq 1$ Bev and becomes completely negligible at energies less than 0.6 Bev/nucleon. This is illustrated in Fig. 5. This correction has been calculated for intervals I and II ($E > 883$ Mev/nucleon) and III (570–883 Mev/nucleon). The effect of applying this correction is to remove the asymmetry in the ionization distribution. Thus the pulse-height distributions from both detectors should be approximately Gaussian in the energy-sensitive region. If now the intervals have been selected so that there are equal numbers of alphas per interval after the Williams-Landau asymmetry has been removed, then this number should represent a

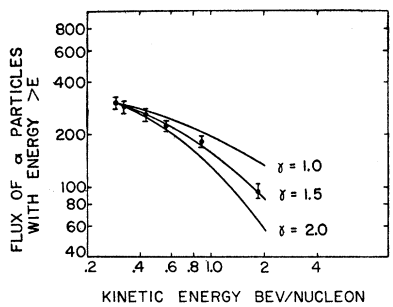

FIG. 10. Integral energy spectrum of primary alpha particles. The point at 1.7 Bev/nucleon is based on $\lambda = 41°$ data.

good approximation to the actual number of particles in the energy interval since the loss to neighboring intervals will tend to be balanced by the gain from these intervals. The energy spectrum data are summarized in Table I. It is seen that this condition has been well satisfied in intervals 3 and 4 but the value of N_α falls off in intervals 5 and 6. A correction factor was computed by the synthesis of the pulse-height distributions. This correction factor was never greater than 10%. This gives added confidence that this method of analysis has not introduced major errors in the derivation of the energy spectrum. In a similar manner the contributions of intervals I and II to III were computed. This is necessary because of the great difference in N_α in the three intervals. These corrections have all been applied with the Williams-Landau correction in column 6 of Table I. In column 7, N_α is converted to a vertical flux value and in Column 8 the δ-ray correction and the correction for nuclear absorption in the telescope and in the atmosphere above the telescope have been applied. In column 9 the values for the differential energy spectrum are given. The flux data for Flight I are also included in Table I. Figures 9 and 10 give the points obtained for the differential and integral energy spectrum. In each graph the high-energy point makes use of $J_{0\alpha}$ at 41°N. A geomagnetic cutoff of 1.65 Bev/nucleon has been calculated for this point. This is the only point dependent on geomagnetic theory. Also in Fig. 9 are the experimental points measured by Waddington[6] at $\lambda=55°$ using emulsion. The general agreement is good. The data in Figs. 9 and 10 have been fitted with a curve of the form

$$J_{0\alpha}(\geqq E)=c/(1+E)^\gamma, \qquad (4)$$

where E=kinetic energy in Bev. It is found that a best fit is obtained for $\gamma=1.4\pm0.2$ and $c=431$.

The vertical α flux values at $\lambda=55°$ and 41° are

$J_{0\alpha}(E>285$ Mev/nucleon)
$=306\pm24$ particles/m²-sec-sterad (without fragmentation correction),

$J_{0\alpha}(E_1)=96\pm9$ particles/m²-sec-sterad;

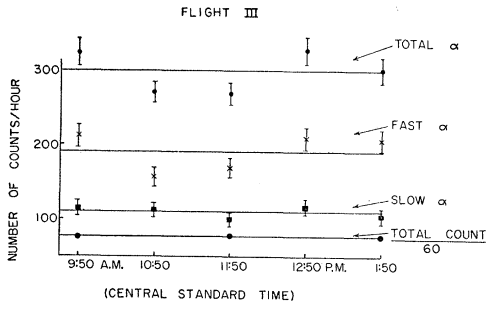

FIG. 11. Observed hourly rates for total alpha, fast alpha ($E>800$ Mev/nucleon), slow alpha ($E<800$ Mev/nucleon), and total telescope rate. Time is central standard time.

where E_1=vertical geomagnetic cutoff in Bev/nucleon at 41°.

When the fragmentation correction is applied,

$J_{0\alpha}(E>285$ Mev/nucleon)$=292\pm25$ particles/m²-sec-sterad,

$J_{0\alpha}(E_1)=87\pm9$ particles/m²-sec-sterad.

Because of a gain shift caused by repairs just prior to launching, it was not possible to say anything concerning the geomagnetic cutoff at $\lambda=55°$ except that it is less than 285 Mev/nucleon.

Table II provides a summary of α flux measurements [2,3,6,11–16] at $\lambda=41°$ and 55°. The over-all agreement is quite good.

TABLE II. Summary of α particle flux measurements at $\lambda=55°$N and 41°N.

Method	Author and reference	Flux (particles per m²-sec-sterad)
	$\lambda=41°$	
Proportional counter	Perlow[a]	110±20
Čerenkov counter and cloud chamber	Linsley[b]	88±8
Čerenkov counter	Horowitz[c]	99±16
Čerenkov counter	Webber-McDonald[d]	82±9
Double scintillation counter	Bohl[e]	90±10
Scintillation counter and Čerenkov counter	Present experiment	96±9
	$\lambda=55°$	
Scintillation counter	Ney and Thon[f]	340
Proportional counter	Davis *et al.*[g]	320±40
Cloud chamber	McDonald[h]	240±40
Emulsion	Waddington[i]	320±36
Čerenkov counter and scintillation counter	Present experiment	305±25

[a] See reference 11.
[b] See reference 12.
[c] See reference 2.
[d] See reference 3.
[e] See reference 13.
[f] See reference 14.
[g] See reference 15.
[h] See reference 16.
[i] See reference 6.

VIII. TIME VARIATION

One of the advantages of the Čerenkov—scintillation counter combination is in the study of time variations of the various components and a determination of the energy interval giving rise to this variation. A plot of the observed hourly rates for total apha-particle intensity, fast alphas ($E>900$ Mev), slow alphas ($E<900$ Mev) and total telescope rate is given in Fig. 11. It is

[11] Perlow, Davis, Kissinger, and Shipman, Phys. Rev. **88**, 321 (1952).
[12] J. Linsley, Phys. Rev. **101**, 826 (1956).
[13] L. Bohl, thesis, University of Minnesota, 1954 (unpublished).
[14] E. P. Ney and D. M. Thon, Phys. Rev. **81**, 1068 (1951).
[15] Davis, Caulk, and Johnson, Phys. Rev. **101**, 800 (1956).
[16] F. B. McDonald, thesis, University of Minnesota, 1955 (unpublished).

felt that the data are consistent with no time variation over the period at altitude. However, it is suggestive that the slight increase around 12:30 (central standard time) occurs at the same approximate time as noted by Ney and Thon,[14] Yngve,[17] and Anderson, Frier, and Naugle.[18] It is planned to repeat this experiment with an apparatus having a greater geometric factor. Simpson[19] has made available the neutron data for July 7, 1955 from Climax, Colorado. There are no observed fluctuations during the period of the flight and the neutron counting rate is in close agreement with the yearly mean—illustrating that this was a "normal cosmic-ray day."

IX. ENERGY RESPONSE OF ČERENKOV COUNTER TO FAST MULTIPLY-CHARGED PARTICLES

The theoretical dependence on Z and β of the Čerenkov radiation is given by Eq. (2). However, this equation was not used explicitly in deducing the energy spectrum. It was assumed merely that the radiation was Z dependent and decreased monotonically as the velocity decreased. It is of interest to measure the Z and β response of the Čerenkov counter to fast multiply-charged particles. By comparing the relativistic proton and alpha distribution ($E>2$ Bev/nucleon) it was established that for $\beta\approx 1$, the radiation varied as Z^2 within the 7% experimental error. The β dependence of the Čerenkov radiation can be studied by noting the position of the peak in the Čerenkov distribution in the various ionization intervals given in Fig. 7. These experimental points are plotted in Fig. 1. In Fig. 12 they are replotted as function of E. In both cases the experimental points have been normalized to the theoretical curve at interval I ($\bar{E}=3$ Bev). Agreement with the theoretical curve is excellent for the higher values of E. However, at levels near the Čerenkov threshold there appears to be some fluorescence. This is not unexpected.

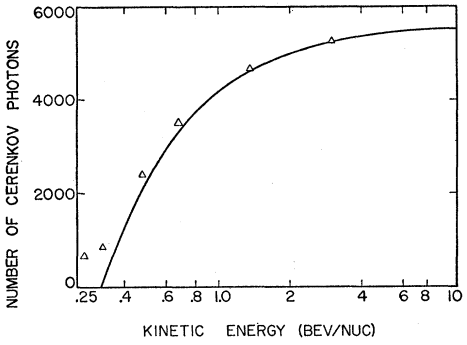

FIG. 12. Plot of Čerenkov light *vs* kinetic energy/nucleon for alpha particles. The experimental points have been normalized to the theoretical curve at the highest experimental point.

X. CONCLUSIONS

It is believed that the method described in this paper is equally applicable to the proton and to the light and medium cosmic-ray components. It is interesting to note that at 300 Mev/nucleon, the alpha spectrum is still rising rapidly toward lower energies. It is planned to extend these measurements to higher latitudes in the near future.

XI. ACKNOWLEDGMENTS

The author wishes to express his appreciation to the Office of Naval Research and to Winzen Research of Minneapolis, Minnesota, for the excellent balloon services that were provided, and to Dr. J. A. Van Allen for discussing this work critically and offering many valuable comments.

[17] V. H. Yngve, Phys. Rev. **92**, 428 (1953).
[18] Anderson, Frier, and Naugle, Phys. Rev. **94**, 1317 (1954).
[19] J. A. Simpson, University of Chicago (private communication).